Title

A method of alternating characteristics with application to advection-dominated environmental systems

Journal

Computational Geosciences, 22(3)

ISSN

1420-0597

Authors

Georgiou, Katerina
Harte, John
Mesbah, Ali
et al.

Publication Date

2018-06-01

DOI

10.1007/s10596-018-9729-5

Peer reviewed

A method of alternating characteristics with application to advection-dominated environmental systems

Katerina Georgiou[1,2] · John Harte[3] · Ali Mesbah[1] · William J. Riley[2]

1 Department of Chemical and Biomolecular Engineering, University of California, Berkeley, CA 94720, USA 2 Earth and Environmental Sciences, Lawrence Berkeley National Laboratory, 1 Cyclotron Rd., 74R316C, Berkeley, CA 94720, USA 3 Energy and Resources Group, University of California, Berkeley, CA 94720, USA

Abstract

We present a numerical method for solving a class of systems of partial differential equations (PDEs) that arises in modeling environmental processes undergoing advection and biogeochemical reactions. The salient feature of these PDEs is that all partial derivatives appear in linear expressions. As a result, the system can be viewed as a set of ordinary differential equations (ODEs), albeit each one along a different characteristic. The method then consists of alternating between equations and integrating each one step-wise along its own characteristic, thus creating a customized grid on which solutions are computed. Since the solutions of such PDEs are generally smoother along their characteristics, the method offers the potential of using larger time steps while maintaining accuracy and reducing numerical dispersion. The advantages in efficiency and accuracy of the proposed method are demonstrated in two illustrative examples that simulate depth-resolved reactive transport and soil carbon cycling.

Keywords: Soil biogeochemical cycles · Reactive transport modeling · Numerical methods · Partial differential equations · Method of characteristics

1 Introduction

Typically, models of environmental processes must be solved over long time horizons and over many spatial grid points to make projections that establish how external stimuli might affect the state of a system [1, 2, 5, 14, 36, 41, 42, 46, 48]. In addition, multi-model ensembles are often used due to uncertainty in model structure and parameter values to obtain not only one projection but also a range depicting its uncertainty [17, 23, 46, 48]. Such simulations require considerable computational resources, especially since the solutions must be obtained over sufficiently small time steps to maintain accuracy and avoid errors due to numerical dispersion. There is, thus, an ongoing need for improving the numerical tools used to solve spatially and temporally resolved reactive transport models over large space and time horizons.

The type of equations we are concerned with here is typical of those arising in environmental systems in which one or more components undergo advective transport in addition to chemical or biological reactions. Such equations occur, for example, in modeling of pollutant transport through a

porous, reactive medium or in modeling of soil carbon cycling where leaching processes transport dissolved organic carbon vertically through the soil profile [1, 16, 22, 23, 36, 41, 42, 45]. These types of systems give rise to equations of the form

$$\frac{\partial u_i}{\partial t} = f_i\,(t, x, u_1, \ldots, u_n) - c_i\,(t, x)\,\frac{\partial u_i}{\partial x}, \text{ for } i = 1, \ldots, n \tag{1}$$

where ui is the concentration of the ith component of the system, fi(t, ui,...,un) is the nonlinear function that encodes the reactions governing ui, and ci(t, x) is the advective velocity (e.g., of water through the soil profile). We then have equations in which the partial derivatives with respect to space and time appear linearly for each ith component, modified only by coefficients. We note that the advective velocity (ci) may, in fact, be spatially varying, so we present an extension of our method to accommodate this dependence. These equations comprise a system of coupled, hyperbolic partial differential equations (PDEs), and although they can be solved numerically via standard methods [11, 12, 20, 26, 33, 35, 43], the specific form that arises in environmental processes is often amenable to a natural and simpler numerical solution as a set of ordinary differential equations (ODEs) along a customized grid by a suitable adaptation of the method of characteristics [12, 13].

In essence, the proposed method transforms the above coupled PDEs into coupled ODEs, each one propagating along its own characteristic, and alternates in solving each equation by step-wise numerical integration along its corresponding characteristic. The method takes advantage of the fact that the solutions of advection-dominated PDEs are generally much smoother along their characteristics than they are in the time direction [12, 49]. This allows for larger time steps in a simulation without a loss of accuracy and reduces the numerical dispersion present in many Eulerian methods [12, 43]. Additionally, since the grid is uniquely defined by the physics (via the characteristics) of the system, the proposed method is not susceptible to grid orientation effects, in contrast to finite-difference methods. We implement a numerical integration using the implicit Euler method to achieve better accuracy and stability compared to the explicit Euler scheme [24, 33]. For specific forms of the governing equations, the method can be generalized to more than one spatial dimension.

In the next section, the proposed method, termed the method of alternating characteristics (MAC), is described for a system of two, three, or more characteristic directions and extended to spatially variable characteristic directions and more than one spatial dimension, as well as to systems where both advection and diffusion are present. We then present, in Section 3, two example applications that arise in modeling reactive transport and depth-resolved soil carbon cycling. We solve each system of equations using the method of alternating characteristics and standard methods for

approximating PDEs (e.g., finite differences). We compare the solutions in terms of accuracy, speed, and robustness and explore advantages of the proposed method. While optimized integration schemes may outperform our chosen standard, we emphasize that the goal here is to illustrate that the physics of advection-dominated environmental systems is uniquely suited for the proposed method and that further optimization may be necessary. Finally, concluding remarks are given in Section 4.

2 Method of alternating characteristics

In general, for a given component (i), the partial differential equation

$$\frac{\partial u_i}{\partial t} = f_i\,(t, x, u_i, \ldots, u_n) - c_i\,(t, x)\,\frac{\partial u_i}{\partial x}$$

that is linear in the spatial partial derivative can be turned into the equivalent ordinary differential equation

$$\frac{\mathrm{d}u_i}{\mathrm{d}t} = \frac{\partial u_i}{\partial t} + \frac{\partial u_i}{\partial x}\frac{\mathrm{d}x}{\mathrm{d}t} = f_i\,(t, x, u_i, \ldots, u_n)$$

along the characteristic x(t) defined by dx(t) dt = ci(t, x) [12, 33]. For a system with two or more PDEs as above, the basic idea of the MAC is to alternate between (ordinary) integrations along characteristics, each time integrating step-wise the corresponding ODE equation along its respective characteristic. We first focus on the case where ci is constant, in which case, the characteristic is

$$x\,(t) = x_0 + c_i t$$

and will be referred to as a constant characteristic direction. The method is described in detail, first for a system with two constant characteristic directions, followed by a discussion for extending this method to systems with more general (e.g., spatially varying) characteristic directions as well as systems with more than two characteristics. Our interest is mainly in one spatial dimension; in Section 2.4, we remark and discuss special cases where the method can be extended to more than one spatial dimension.

In the developments that follow, we adopt the commonly used compact notation of denoting partial derivatives ∂u ∂x by ux and ∂u ∂t by ut .

2.1 System of two constant characteristic directions Consider a system of two PDEs as in Eq. 1, with constant advective velocities (ci) where i ∈ {1, 2}. Without a loss of generality, we can assume that one of the two is equal to zero and the other normalized to 1. Thus, simplifying the notation for illustration, we consider two scalar functions, u(t, x) and v(t, x), satisfying

$$u_t = f(t, x, u, v) - u_x \tag{2a}$$

$$v_t = g(t, x, u, v) \tag{2b}$$

Along the characteristic of v (i.e., $x^v(t) = x_0$ since $\dot{x}^v(t) = \frac{dx^v(t)}{dt} = 0$, where the superscript denotes the dependent variable to which the characteristic belongs), Eq. 2b becomes the ODE

$$\frac{dv}{dt} = g(t, x_0, u, v)$$

where the function g depends on u(t, x0). However, u(t, x0) is not known ahead of time and depends on values of u(t, x) at nearby points in the spatial direction, via Eq. 2a. In turn, Eq. 2a can be written as an ODE when solved along its corresponding characteristic,

$$\begin{aligned}\frac{du}{dt} &= u_t + u_x \dot{x}^u \\ &= f(t, x_0 + t, u, v)\end{aligned}$$

along the line $\dot{x}^u(t) = 1$, or, equivalently, along $x^u(t) = x0 + t$. This is so because Eq. 2a has the character of a wave equation [33]. Here, the function (f) depends on v(t, x0+t) which evolves in time and space via Eq. 2b. We summarize that Eq. 2b can be solved as an ODE along the characteristic $\dot{x}^v = 0$, while Eq. 2a can be solved as an ODE along $\dot{x}^u = 1$. We briefly note that along the line $\dot{x}^v = 1$, Eq. 2b is no longer an ODE, but rather, it becomes

$$\begin{aligned}\frac{dv}{dt} &= v_t + v_x \dot{x}^v \\ &= g(t, x_0 + t, u, v) + v_x.\end{aligned}$$

Thus, the wave nature of one of the two equations complicates matters and we cannot reduce the system to a corresponding system of ODEs unless we alternate between the directions of the two characteristics: $\dot{x}^u = 1$ to solve for u and $\dot{x}^v = 0$ for v. By developing a customized grid, we can alternate between these characteristic directions and solve the system as two ODEs, rather than as numerically approximated PDEs.

For the particular example above, with characteristics $\dot{x}^v = 0$ and $\dot{x}^u = 1$, the corresponding grid is shown in Fig. 1a, where we can solve the ODE for u diagonally and for v horizontally. We can only solve each over the time step t since we must update the value of both u and v at the nodes of the grid for successive points in time.

Thus, the numerical scheme amounts to updating the value of u and v at the node points, as follows:

Fix t and consider successively the points in time $t \in \{0, t, 2t, \ldots, kt, \ldots\}$ and the corresponding values of

$u_{k,l} = u(k\Delta t, l\Delta x)$ and $v_{k,l} = v(k\Delta t, l\Delta x)$

In the case of Eq. 2a, $\Delta x = \Delta t$ since one characteristic is $x^u(t) = \text{constant} + t$ at the corresponding spatial coordinates. Starting from given boundary values

$$\{u_{0,l}, v_{0,l} | l = 0, 1, 2, \ldots\} \text{ and } \{u_{k,0} | k = 1, 2, \ldots\}$$

compute recursively for increasing values of $k \geq 0$,

$$u_{k+1,l} = u_{k,l-1} + f(u_{k,l-1}, v_{k,l-1})\Delta t, \text{ for } l = 1, 2, \ldots \quad (3a)$$

$$v_{k+1,l} = v_{k,l} + g(u_{k,l}, v_{k,l})\Delta t, \text{ for } l = 0, 1, 2, \ldots \quad (3b)$$

This constitutes the *explicit* (forward) Euler method and is shown schematically for $u_{k+1,l}$ and $v_{k+1,l}$ in Fig. 1b.

A small modification of the approach allows the usage of the implicit (backward) Euler method for solving the differential equations along the characteristics. More specifically, replace Eq. 3, by the following implicit equations:

$$u_{k+1,l} = u_{k,l-1} + f(u_{k+1,l}, v_{k+1,l})\Delta t, \text{ for } l = 1, 2, \ldots \quad (4a)$$

$$v_{k+1,l} = v_{k,l} + g(u_{k+1,l}, v_{k+1,l})\Delta t, \text{ for } l = 0, 1, 2, \ldots \quad (4b)$$

These can then be solved by a fixed-point iteration

$$u^{(i+1)}_{k+1,l} = u_{k,l-1} + f\left(u^{(i)}_{k+1,l}, v^{(i)}_{k+1,l}\right)\Delta t, \text{ for } l = 1, 2, \ldots \quad (5a)$$

$$v^{(i+1)}_{k+1,l} = v_{k,l} + g\left(u^{(i)}_{k+1,l}, v^{(i)}_{k+1,l}\right)\Delta t, \text{ for } l = 0, 1, 2, \ldots \quad (5b)$$

starting from

$$u^{(0)}_{k+1,l} = u_{k,l-1} \text{ and } v^{(0)}_{k+1,l} = v_{k,l}.$$

The above system of equations is a vectorial equation of the form

$$\begin{bmatrix} u^{(i+1)}_{k+1,l} \\ v^{(i+1)}_{k+1,l} \end{bmatrix} = F\left(\begin{bmatrix} u^{(i)}_{k+1,l} \\ v^{(i)}_{k+1,l} \end{bmatrix}\right)$$

where the map

$$F\left(\begin{bmatrix} \mathbf{u} \\ \mathbf{v} \end{bmatrix}\right) = \begin{bmatrix} u_{k,l-1} + f(\mathbf{u}, \mathbf{v})\Delta t \\ v_{k,l} + g(\mathbf{u}, \mathbf{v})\Delta t \end{bmatrix}.$$

It is clear that for sufficiently small Δt, F is Lipschitz continuous with the Lipschitz constant $L < 1$, since

$$\left\| F\left(\begin{bmatrix} \mathbf{u_1} \\ \mathbf{v_1} \end{bmatrix}\right) - F\left(\begin{bmatrix} \mathbf{u_0} \\ \mathbf{v_0} \end{bmatrix}\right) \right\| = \left\| \Delta t \begin{bmatrix} f(\mathbf{u_1}, \mathbf{v_1}) - f(\mathbf{u_0}, \mathbf{v_0}) \\ g(\mathbf{u_1}, \mathbf{v_1}) - g(\mathbf{u_0}, \mathbf{v_0}) \end{bmatrix} \right\| < \left\| \begin{bmatrix} \mathbf{u_1} \\ \mathbf{v_1} \end{bmatrix} - \begin{bmatrix} \mathbf{u_0} \\ \mathbf{v_0} \end{bmatrix} \right\|.$$

Therefore, the fixed-point iteration in Eq. 5 converges. In the simulations, a fixed number of steps for the iteration are deemed sufficient, and it is observed that they give an improvement over the standard explicit Euler method.

The proposed method can be applied to a system of more than two equations without any modification, provided they share the same two characteristics. In fact, this is not unusual in many natural systems. For example, in soil, some chemical components may experience advection (i.e., leaching) with a particular gravity- or pressure-driven water velocity, while other components experience no leaching [1, 36]. In that case, a subset of equations can be solved along the characteristic dictated by the magnitude of the water advective velocity (i.e., $\dot{x}$ (t) = c for some value c), while the remaining equations can be solved along constant values of x (i.e., $\dot{x}$ (t) = 0).

If, however, there are more than two characteristics, e.g., for three dependent variables (u, v and w), we need to adjust the grid appropriately and possibly interpolate values of some of the dependent variables. This scenario will be discussed below, along with the case where the velocities (and therefore the characteristics) vary spatially.

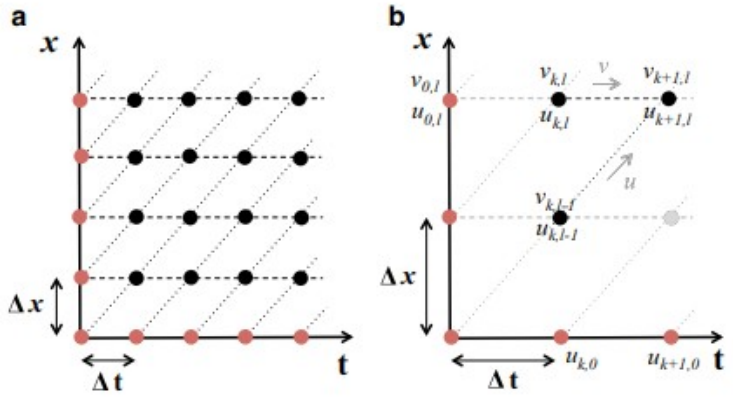

Fig. 1 Schematic of a customized grid for propagating the integration along two constant characteristics, such as those arising in Eq. 2a, b. **a** Characteristic directions $x^v(t) = x_0$ (dashed horizontal lines; $\dot{x}^v = 0$) and $x^u(t) = t + x_0$ (dotted diagonal lines; $\dot{x}^u = 1$) for solving the system of PDEs in Eq. 2a, b . Boundary and initial conditions are depicted in red. **b** Propagating the integration along two characteristics using the explicit or implicit Euler methods (as in Eqs. 3a, b or 4a, b respectively) to obtain $u_{k+1,l}$ and $v_{k+1,l}$, where initial ($u_{0,l}$, $v_{0,l}$) and boundary ($u_{k,0}$) conditions are shown in red

2.2 System of three or more characteristic directions

Consider the case of three coupled PDEs

$$u_t = f(u, v, w) - u_x \tag{6a}$$
$$v_t = g(u, v, w) \tag{6b}$$
$$w_t = h(u, v, w) - cw_x. \tag{6c}$$

Once again, and without a loss of generality, one velocity is normalized to 1 and another to 0, and the remaining advective velocity is c.

We may form a grid as before on which to alternate directions and integrate Eqs. 6a and 6b. However, in order to update the values of w, we need to integrate Eq. 6c along a different characteristic. If the advective velocity of w (c; denoted $\dot{x}_w$) is an integer (i.e., integer multiple of $\dot{x}_u$), the grid points

dictated by the advective velocities of u and v are sufficient, namely the (uv) grid as defined in Section 2.1. Then, all dependent variables can be consistently determined on these points. If, however, c is not an integer multiple of the advective velocity of u, the value of w needs to be interpolated accordingly. More specifically, the value of w can be computed by integrating Eq. 6c at points that fall outside the grid and those values can then be used to approximate w on the (uv) grid (see Fig. 2). For instance, the values of w at points (t, x1) and (t, x2) can be used to linearly interpolate the value of w at (t, x), as shown in Fig. 2. We note that, in principle, the interpolation should be of at least the same order as the integration scheme, which is here of first order.

In this way, following the rationale in the MAC, we can again use ordinary integration along characteristics as specified by the physics of the system. The choice of which equations to normalize and, thereby, determine the grid on which to evaluate the parameters may have an impact on the numerical accuracy. Further analysis is needed to assess the optimal choice.

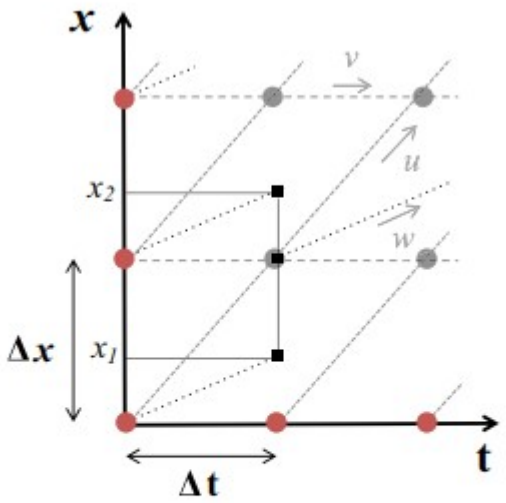

Fig. 2 Schematic of a customized grid for propagating the integration along three characteristic directions—$\dot{x}^u = 1$, $\dot{x}^v = 0$, and $\dot{x}^w = c$, as in Eq. 6a–c —with interpolation of integrated values of $\dot{x}^w = c$ from spatial locations $(\Delta t, x_1)$ and $(\Delta t, x_2)$ in-between existing grid points (shown as black squares). The order of interpolation should be of at least the same order as the integration scheme. The integration then proceeds as before, alternating ordinary integration of each equation, along the customized grid. Boundary conditions are shown in red

2.3 System with spatially varying characteristic directions

On account of the underlying physics, the advective velocity may vary in space and time, i.e., as c(t, x) [16, 23, 41, 42]. For example, the number and size of pore spaces in soil (and consequently, the bulk density) through which water flows may vary with depth [1, 29, 36, 47]. Given mass balance considerations and no accumulation, this implies that the velocity changes

with depth as the flow path changes. Additionally, leaching may vary according to the amount of water entering the soil (e.g., due to changes in precipitation) at a particular point in time [15, 29, 36, 47]. Thus, we can see that the method presented above often needs to be extended to the case of variable characteristic directions.

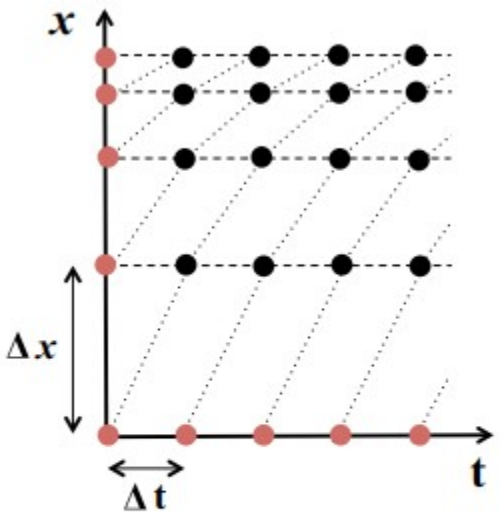

Fig. 3 Schematic of a customized grid for propagating the integration along two varying characteristics, such as those arising in systems with spatially variable advective velocity. In this example, $\dot{x}^v = 0$ (dashed horizontal lines) and $\dot{x}^u = c(x)$ (dotted diagonal lines). The step Δx varies with x and is dictated by $c(x)\,\Delta t$. Boundary conditions are shown in red

For illustration purposes, we consider the case where the advective velocity is only spatially variable; i.e., it is c(x). Figure 3 displays a suitable grid for the numerical scheme to solve an example with depth-varying advective velocity. Of particular interest, conferring advantages to the MAC may be the case where the depth-varying velocity changes abruptly between layers (rough coefficients in the PDEs) as dictated by the underlying physics. An example of such a case will be simulated and discussed in Section 3.1.

In principle, it is also possible to include temporal variation, either as c(t) or c(t, x) depending on the system. However, in such a case, the suitable grid may be complicated or may require additional interpolation. Since MAC is a first-order method, in principle, any approximation should be at least of first order. In practice, however, simplifications are often employed that ignore this time dependence. In the case of soil carbon modeling, a temporally averaged water flux is often used, calculated based on monthly or annually averaged precipitation [1, 29]. Hence, the velocity is taken as a constant in time and the use of a temporally varying velocity may depend on the timescale of interest.

2.4 Characteristics in more than one spatial dimension

The basic property that allows adapting the method of characteristics to a hyperbolic system of PDEs is the ability to generate a customized lattice (grid) where the spatial and temporal derivatives can be numerically approximated, consistently and simultaneously, for each of the equations of the hyperbolic system. For this to be the case, it is important that the characteristics display a suitable spatial invariance. The type of equations that arises in environmental models (e.g., of biogeochemical processes) is often simple enough to justify such a property.

Once again, we consider two dependent variables, u and v. We consider two spatial dimensions with coordinates designated as x and y and PDEs of the form

$$u_t = f(t, x, y, u, v) - c_1(x)\, u_x - c_2 u_y, \tag{7a}$$

$$v_t = g(t, x, y, u, v). \tag{7b}$$

This set of equations arises naturally in instances where two components (with concentrations, u and v) chemically interact, while one of the two advects (e.g., component u leaches through the soil) and the other is stationary (e.g., v is adsorbed to the soil matrix). The advective velocities in the x and y directions may depend on different physical factors. For example, the velocity in the y (horizontal) direction could be driven by a constant pressure gradient, possibly due to a nearby river or sloped catchment [15, 31, 37, 47]. The gravity-driven velocity in the x (vertical) direction, on the other hand, may be a function of the depth (rather than being constant) due to differing medium properties (e.g., porosity) with depth [1, 36]. In this instance, the characteristics for component u (distinguished by a superscript) are defined by

$$\dot{x}^u = c_1(x) \tag{8a}$$

$$\dot{y}^u = c_2, \tag{8b}$$

and for component v,

$$\dot{x}^v = 0 \tag{9a}$$

$$\dot{y}^v = 0. \tag{9b}$$

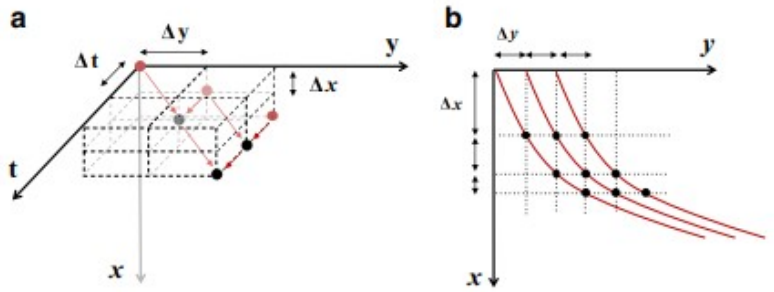

Fig. 4 Schematic of a customized lattice for two spatial dimensions, where the integration is propagated along distinct characteristics for dependent variables u and v, as arising in Eqs. 7–9. **a** Characteristic directions $\dot{x}^u = c_1(x)$ and $\dot{y}^u = c_2$ for variable u (red diagonal arrows) and $\dot{x}^v = 0$ and $\dot{y}^v = 0$ for variable v (red arrows perpendicular to xy plane) are used to form the customized lattice and propagate ordinary integration of the corresponding coupled ODEs as in Eq. 10a, b. **b** The characteristic curves of u are projected on the xy plane (shown in red), and the dots represent the projection of the characteristic curves of v. Here, the characteristic $\dot{x}^u = c_1(x)$ is spatially varying, as in Eqs. 7a, b and 8a, b

As seen in Fig. 4a, a customized lattice, where spacing is regular in the y direction and adjustable in the x direction, provides a grid that allows integration of ODEs numerically along corresponding characteristics in a suitable manner. The curves in Fig. 4b represent the projection of the characteristics of u (that may be spatially variable, as shown) on the (xy) plane, whereas the dots represent the projection of the characteristics of v. The lattice consists of points

$$(t, x, y) = (k\Delta t, \sum_{i=1}^{l} \Delta x_i, m\Delta y)$$

and the corresponding variables for the numerical scheme are labeled accordingly as uk,l,m and vk,l,m. Along the characteristics in Eqs. 8a, b and 9a, b the ordinary difference equations for the explicit Euler scheme take the form

$$u_{k+1,l,m} = u_{k,l-1,m-1} + f(u_{k,l-1,m-1}, v_{k,l-1,m-1})\Delta t \quad (10a)$$
$$v_{k+1,l,m} = v_{k,l,m} + g(u_{k,l,m}, v_{k,l-1,m-1})\Delta t, \quad (10b)$$

respectively, where u and v are computed recursively for increasing values of k ≥ 0, starting from given boundary conditions

$$\{u_{0,l,m}, v_{0,l,m} \,|\, l = 0, 1, 2, \ldots, m = 0, 1, 2, \ldots\} \text{ and}$$
$$\{u_{k,l,0} \,|\, k = 0, 1, 2, \ldots, l = 0, 1, 2, \ldots\}$$

Similarly, the implicit Euler method, together with a fixed-point iteration scheme, can be employed using f and g evaluated at (uk+1,l,m, vk+1,l,m).

In more general situations, when a family of characteristics cannot be found that meets at the nodes of a lattice, advantages may still be drawn from a customized grid in conjunction with approximation schemes to interpolate at in-between points as discussed earlier.

2.5 System with diffusion and advection

For many of the physical processes that we consider, it is expected that a small amount of diffusion will be present; e.g., that dissolved organic carbon will diffuse through the porous soil media. Thus, a more accurate model may be of the form

$$\frac{\partial u_i}{\partial t} = f_i\,(t, x, u_i, \ldots, u_n) - c_i\,(t, x)\,\frac{\partial u_i}{\partial x} + \varepsilon_i \frac{\partial^2 u_i}{\partial x^2}.$$

Numerically, we need to introduce $\left(\varepsilon_i \frac{\partial^2 u_i}{\partial x^2}\right)$ as an additional term in Eqs. 3a, b and 4a, b. A natural choice is to estimate the second partial derivatives with respect to x by either

$$\frac{\partial^2 u}{\partial x^2} \approx \frac{\frac{u_{k,l}-u_{k,l-1}}{\Delta x} - \frac{u_{k,l-1}-u_{k,l-2}}{\Delta x}}{\Delta x} = \frac{u_{k,l} - 2u_{k,l-1} + u_{k,l-2}}{\Delta x^2} \tag{11a}$$

and

$$\frac{\partial^2 v}{\partial x^2} \approx \frac{v_{k,l+1} - 2v_{k,l} + v_{k,l-1}}{\Delta x^2} \tag{11b}$$

or, alternatively,

$$\frac{\partial^2 u}{\partial x^2} \approx \frac{u_{k+1,l} - 2u_{k+1,l-1} + u_{k+1,l-2}}{\Delta x^2} \tag{12a}$$

and

$$\frac{\partial^2 v}{\partial x^2} \approx \frac{v_{k+1,l+1} - 2v_{k+1,l} + v_{k+1,l-1}}{\Delta x^2} \tag{12b}$$

for explicit and implicit difference schemes, respectively. The approximation of the diffusion term can also be accomplished via finite volume methods [21, 26, 35]. If we use Eq. 11a, b we need to modify Eq. 3a, b as follows:

$$u_{k+1,l} = u_{k,l-1} + f\left(u_{k,l-1}, v_{k,l-1}\right)\Delta t + \varepsilon_u \left(\frac{u_{k,l} - 2u_{k,l-1} + u_{k,l-2}}{\Delta x^2}\right)\Delta t, \text{ for } l = 1,2,\ldots$$

$$v_{k+1,l} = v_{k,l} + g\left(u_{k,l}, v_{k,l}\right)\Delta t + \varepsilon_v \left(\frac{v_{k,l+1} - 2v_{k,l} + v_{k,l-1}}{\Delta x^2}\right)\Delta t, \text{ for } l = 0,1,2,\ldots$$

If we use Eqs. 4a, b and 12a, b instead, the difference equations become implicit as both uk+1,l and vk+1,l appear in the expression for the second partial with respect to x. These equations must be solved by relying on a fixedpoint iteration as before. However, since the estimate for the second partial requires x2 in the denominator, the relative sizes of t, x, and ε values are critical and a Lipschitz constant of less than 1 may not be possible to guarantee. This appears to be the case when the magnitude of t ≈ x and x is small relative to the ε values.

3 Applications and results

The MAC is uniquely suited to solve systems where subsets of the chemical constituents experience different advective velocities. Such instances arise naturally in many depth-resolved reactive transport models with flow through a porous, reactive medium, where only a subset of the constituents experience leaching [1, 16, 22, 23, 32, 36, 41, 42]. For example, this encompasses many instances of pollutant transport through soil and extends to models of soil carbon cycling where dissolved organic matter experiences leaching in addition to microbial decomposition and adsorption to mineral surfaces. Earlier method-ofcharacteristics-based ideas [3, 7, 8, 13, 38] have not been applied to this type of system where multiple characteristics must be reconciled and simultaneously utilized on a customized grid, limiting our ability to compare directly to such methods. The efficiency and accuracy (convergence towards the exact solution) of the MAC is therefore compared to a standard finite-difference scheme. More specifically, the first-order, implicit upwind finite-difference scheme (hereafter, FD) is used to allow for a direct comparison with the first-order, implicit Euler method used in the MAC, as detailed in Eqs. 4a, b and 5a, b. For the system in Eqs. 1 and 2a, b, following the discretization uk,l = u(kt, lx) and vk,l = v(kt, lx), the upwind scheme employed can be represented in compact notation as follows:

$$u_{k+1,l}=u_{k,l}+f\left(u_{k+1,l}, v_{k+1,l}\right)\Delta t-\left[c^{+}\left(\frac{u_{k,l}-u_{k,l-1}}{\Delta x}\right)+c^{-}\left(\frac{u_{k,l+1}-u_{k,l}}{\Delta x}\right)\right]\Delta t \qquad (13)$$

where c+ = max (c, 0) and c− = min (c, 0) and, similarly, for vk+1,l with g uk+1,l, vk+1,l [33, 34]. Thus, if c > 0, as is the case in the examples below, c+ = c and c− = 0. This implicit scheme can be solved by a fixed-point iteration, as described in Eqs. 4a, b and 5a, b, as opposed to an explicit scheme where f and g are directly evaluated at (uk,l, vk,l). We note that implicit evaluation of spatial derivatives at tk+1 resulted in additional numerical dispersion. We have therefore restricted our attention to the case where only f and g are implicitly evaluated as in Eq. 13. The upwind finite-difference scheme in Eq. 13 is first order in both space and time. While we consider only first-order schemes here, alternative higher-order schemes can be used for both the MAC and FD, e.g., higher-order Runge-Kutta methods to approximate the ODE in the MAC and, accordingly, for the FD [19, 25]. The performance of the proposed method is highlighted by two examples of typical one-dimensional environmental applications in Sections 3.1 and 3.2.

3.1 Reactive transport through a porous medium

We apply the MAC to simulate depth-resolved, advectiondominated transport in which an unspecified number of substrates (for example, dissolved organic matter or extraneous pollutants) are leached through a porous medium (e.g., soil) while also undergoing reactions with the stationary parent material. Here, we imagine that a substrate flows through the soil profile but can no longer be leached if adsorbed to a mineral surface. In its dissolved and

leachable state, the substrate constitutes the dissolved pool (CD), while in its adsorbed and stationary state, the substratemineral complex makes up the mineral-associated pool (Cq). The adsorption and desorption reaction rate constants are denoted kads and kdes, respectively, and the advective transport is driven by the water velocity (c) through the medium (see Fig. 5). Assuming that a surplus of mineral binding sites (qmax) exists to adsorb the substrate, the temporal and spatial evolution of the two dependent variables is dictated by

$$\frac{\partial C_D(t,x)}{\partial t} = \underbrace{-k_{ads}C_D\left(q_{max}-C_q\right)}_{\text{adsorption}} + \underbrace{k_{des}C_q}_{\text{desorption}} \underbrace{-c\frac{\partial (C_D)}{\partial x}}_{\text{leaching}} \quad (14a)$$

$$\frac{\partial C_q(t,x)}{\partial t} = \underbrace{k_{ads}C_D\left(q_{max}-C_q\right)}_{\text{adsorption}} - \underbrace{k_{des}C_q}_{\text{desorption}} \quad (14b)$$

where all functions depend on time (t) and depth (x). This example is easily extended to the case where there are multiple substrates that undergo reactions, multiple mineral surface types, as well as biological activity in which select substrates are consumed. The key is that only a subset of components undergoes advection, making the MAC uniquely suited to solve such a system.

Without a loss of generality, the parameters kads, kdes, qmax, and c in the above model were assumed to take the values of 1 day−1 kg−1 m3, 1 day−1, 1 kg m−3, and 0.2 m day−1, respectively, recognizing that in real applications, these values are estimated from laboratory experiments; e.g., sorption isotherms for each particular substrate are used to calculate the relevant adsorption and desorption parameters (kads, kdes, qmax) [30]. Figure 6 shows the temporal and spatial evolution of the system in Eq. 14a, b in response to a step input of pollutant of 1 kg m−3 at the surface. The initial condition of both pools is zero pollutant concentration, while the boundary (surface) condition is initially rich in pollutant (imagine a continuous spill) and then free of pollutant (e.g., the spill is contained). Ultimately, the shape of the pollutant profile depends on the initial and boundary conditions, the relative magnitude of the adsorption and desorption rate constants, as well as the advective velocity.

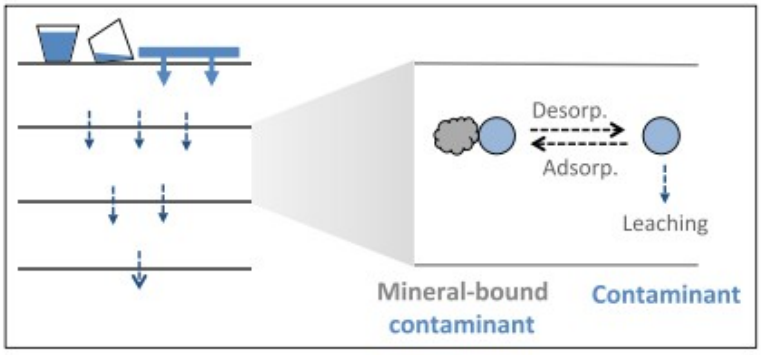

Fig. 5 Schematic of depth-resolved reactive transport where a substrate in the soil profile undergoes advective transport (leaching) and reactions (adsorption and desorption) in time (t) and space (x)—see Eq. 14a, b

We compared the solutions of Eq. 14a, b with time steps (t) ranging from 0.001 to 0.5 days for both the MAC and FD (Fig. 6), where x for MAC is predefined by the nature of the method (i.e., x = ct) and, thus, the same x was adopted for FD to ensure a fair comparison at the same resolution. As aforementioned, we show results from the first-order, implicit upwind finite-difference scheme in Eq. 13 but also note that the first-order, explicit upwind finite-difference scheme was more prone to instabilities, as expected [12, 33]. Comparing the solution of FD across a range of time steps in Fig. 6, where the spatial step size is chosen to allow direct comparison to MAC, we can see that there is substantial numerical dispersion at larger time steps. However, comparing the MAC (Fig. 6, top) to the FD (Fig. 6, bottom), we can clearly see that the MAC maintains performance at coarser grid resolution. This pattern is also illustrated in Fig. 7 where the error (defined as the difference between the solution obtained using t = 0.5 and t = 0.0005) is displayed for both the MAC and FD schemes. The two methods converge at smaller time steps (Δt) < 0.001, and thus Δt = 0.0005 is a good approximation of the true solution [4, 33]. It is observed that the MAC offers a significant advantage, as it allows for faster simulations with larger integration steps that do not sacrifice accuracy.

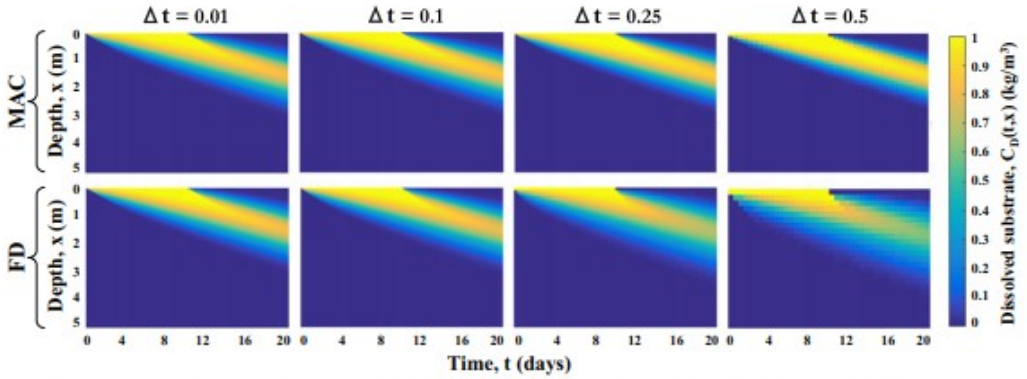

Fig. 6 Solving the system in Eq. 14a, b using the method of alternating characteristics (MAC) (top panels) and the method of finite differences (FD) (bottom panels) with increasing time steps from left to right: Δt = 0.01, 0.1, 0.25, and 0.5 days, respectively. More specifically, the ordinary integration in MAC is performed by the first-order, implicit Euler method. For the FD implementation, the standard first-order, implicit upwind scheme in space and time is used to approximate the corresponding PDEs. The step size (Δx) is predefined for MAC by the nature of the method (i.e., $\Delta x = c\Delta t$), and thus, the same Δx was adopted for FD to ensure a fair comparison at the same resolution. The increased numerical dispersion of the FD solution compared to the MAC solution is observed as the step size increases

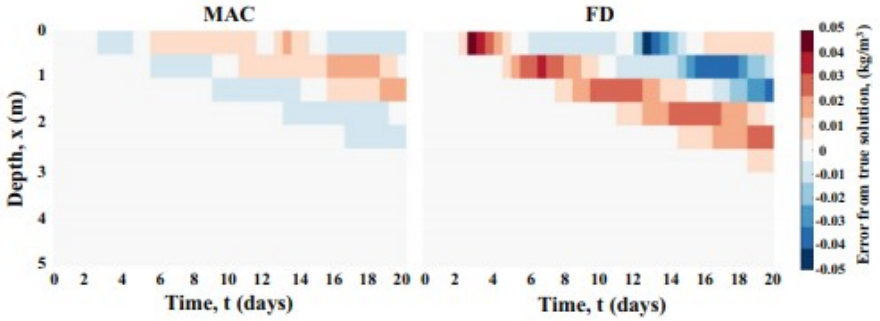

Fig. 7 Numerical dispersion, computed as the difference between the solution using Δt = 0.5 and Δt = 0.0005 days for MAC (left) and FD (right), both with first-order, implicit integration schemes of ordinary and partial derivatives, respectively. Since the solutions of the two methods converge for Δt <0.001, the solution obtained with Δt = 0.0005 days is considered the "true solution" of the system [4, 33]. For consistency, the two methods are compared on a (Δx, Δt) = (0.5 m, 0.5 day) grid. MAC shows significantly lower numerical dispersion

In Fig. 8, we show the simulation runtime and absolute error (defined here as the absolute value of the difference between the solution at each t and the true solution at t = 0.0005; i.e., |estimated − true| as per [4, 33]) as a function of the time step for each of the two methods. While we show the average absolute error (i.e., the L1 norm, |estimated − true|) over space and time in Fig. 8, we also explored the error at select time points, as well as the average squared error (i.e., the L2 norm, (estimated − true) 2) since the choice of norm can be important and should reflect the goal of the computation [4, 44]. We can clearly see that, for this system, the MAC has a distinct advantage over FD and, especially, at larger step sizes. The error is essentially proportional to the step size, as seen in the matching slopes of the MAC and FD lines in Fig. 8b, confirming that we are dealing with first-order numerical methods [33]. By its very nature, the MAC outperforms FD, especially when steep concentration gradients occur. We note that in cases with smoother concentration gradients, the two methods showed similar accuracy, but we did not find the converse, where FD would perform better than the MAC.

While we have thus far explored a numerical example with constant advective velocity, the properties of the medium (e.g., mineralogy and porosity of soil) generally vary with depth [1, 36]. It is also possible to have rough coefficients with depth, for example, in distinct soil horizons (i.e., layers) [30, 36]. A system with heterogeneous coefficients may be more naturally handled by taking advantage of the physics in the MAC solution. A numerical example is presented in Fig. 9, where an abrupt change in the advective velocity occurs with depth. The FD solution results in significant numerical dispersion, especially with steep velocities and large time steps, as seen by comparing the right-hand panels of Fig. 9.

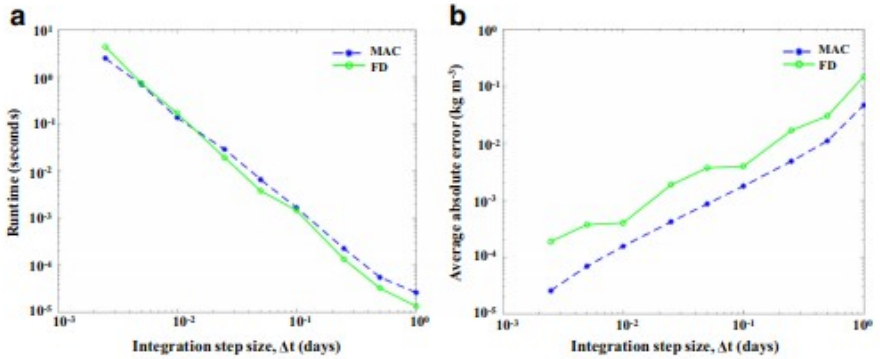

Fig. 8 Comparing the method of alternating characteristics (MAC; dashed lines) to finite differences (FD; solid lines) for the example given in Eq. 14a, b using a range of integration step sizes. Both the MAC and FD are implemented with first-order, implicit integration schemes of ordinary and partial derivatives, respectively. The time step (Δt) is shown, while Δx is predefined for MAC by the nature of the method, and thus, the same Δx was adopted for FD to ensure a fair comparison at the same resolution. **a** Simulation runtime and **b** average absolute value of the error for each Δt compared to the true solution (using an exceedingly small $\Delta t = 0.0005$ days where both methods converge to the same solution). The comparison of CPU time is made on a MacBook Air 2.2 GHz Intel Core i7 processor. For any given accuracy, the MAC can use a significantly larger time step than FD, resulting in a faster runtime

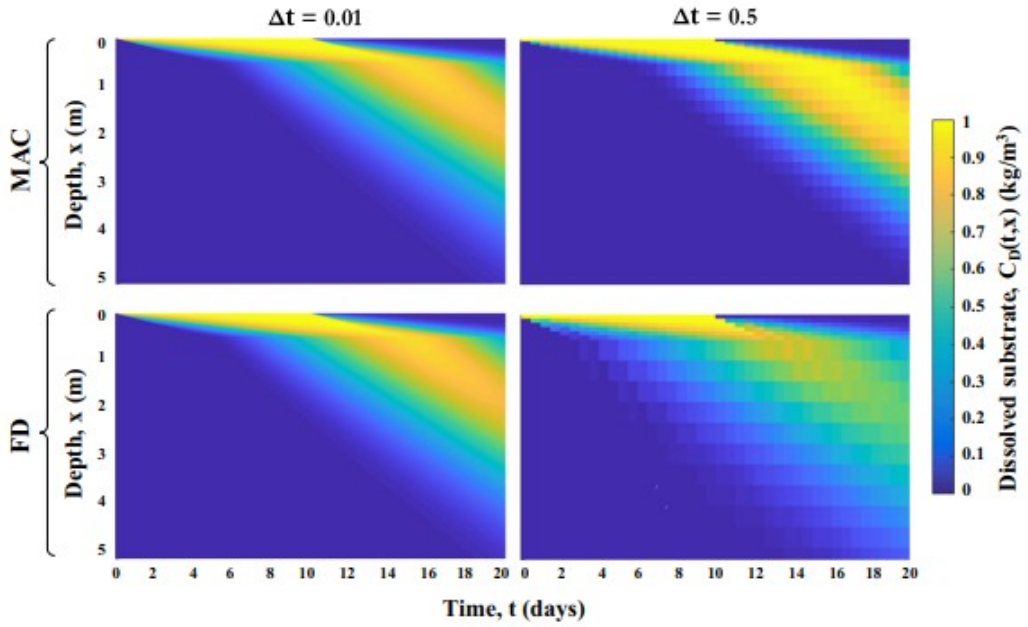

Fig. 9 Solving the system in Eq. 14a, b with an abrupt change in advection velocity with depth (from $c = 0.1$ m day^{-1} to $c = 0.5$ m day^{-1} at 0.5 m depth) using the MAC (top panels) and FD (bottom panels), both with first-order, implicit integration schemes of ordinary and partial derivatives, respectively. The solutions are compared for increasing integration time steps (Δt) and corresponding (Δx) as defined by the MAC, from (left) $\Delta t = 0.01$ to (right) 0.5 days. Significantly more numerical dispersion is observed in the FD solution, especially for steep gradients and larger integration time steps

3.2 Depth-resolved biogeochemical cycling in soil We now apply the MAC to a depth-resolved soil carbon model that includes four pools of organic carbon to a depth of 1 m. These pools include the carbon in polymeric soil organic matter (CS), dissolved organic matter (CD) that leaches down the soil profile with a water transport velocity (c), microbial biomass carbon (CB), and mineralassociated organic matter (Cq). The temporal and spatial evolution of these four dependent variables is dictated by

$$\frac{\partial C_S(t,x)}{\partial t} = \underbrace{-\left(\frac{V_{max} C_B C_S}{K_m + C_S}\right)}_{\text{decomposition}} + \underbrace{k_B C_B}_{\text{mortality}} \tag{15a}$$

$$\frac{\partial C_D(t,x)}{\partial t} = \underbrace{\left(\frac{V_{max} C_B C_S}{K_m + C_S}\right)}_{\text{decomposition}} \underbrace{-\left(\frac{V_{max,U} C_B C_D}{K_{m,U} + C_D}\right)}_{\text{uptake}} \underbrace{-k_{ads} C_D \left(q_{max} - C_q\right)}_{\text{adsorption}} + \underbrace{k_{des} C_q}_{\text{desorption}} \underbrace{- c \frac{\partial (C_D)}{\partial x}}_{\text{leaching}} \tag{15b}$$

$$\frac{\partial C_B(t,x)}{\partial t} = \underbrace{\varepsilon\left(\frac{V_{max,U} C_B C_D}{K_{m,U} + C_D}\right)}_{\text{uptake}} - \underbrace{k_B C_B}_{\text{mortality}} \qquad (15c)$$

$$\frac{\partial C_q(t,x)}{\partial t} = \underbrace{k_{ads} C_D \left(q_{max} - C_q\right)}_{\text{adsorption}} - \underbrace{k_{des} C_q}_{\text{desorption}} \qquad (15d)$$

where all functions depend on time (t) and depth (x). The nonlinear functions of CS, CD, CB, and Cq represent various chemical and biological reactions, including soil organic matter decomposition, uptake of dissolved organic matter into microbial biomass, and organo-mineral adsorption (see schematic in Fig. 10).

We can observe that the system is, in fact, of the same form as the previous example and that of Eq. 1. Here, u and v can be thought of as vector-valued with u = [CD] and v = [CS, CB, Cq], so that there are, again, two corresponding characteristics: $x\dot{}u = c$ and $x\dot{}v = 0$, respectively. Without a loss of generality, we assume values of the parameters as reported in the literature (e.g., [1] and [27]), noting that the relative importance of each term in Eq. 15a–d, as dictated by the values of the parameters, does not affect our conclusions. The parameters Vmax, Km, Vmax,U, Km,U, kB, ε, kads, kdes, qmax, and c take values of 1 day−1, 250 mg C g−1 soil, 0.1 day−1, 0.26 mg g−1, 0.005 day−1, 0.31, 1 (mg g−1)−1 day−1, 0.02 day−1, 1.5 mg g−1, and 0.5 m day−1, respectively (Table 1) [1, 27, 30]. Most of these parameters are derived from laboratory incubations (e.g., kads, kdes, and qmax via sorption isotherm experiments [30] and ε via measurements of microbial growth and respiration [40]), and the remaining parameters are statistically fit to match overall pool sizes (i.e., CS, CD, CB, and Cq) at the field site of interest [1, 27]. We note that the estimation of these parameters, and the final model structure, depends largely on the application. We therefore use these parameters to illustrate the implementation of this method, and this analysis should be taken in that spirit.

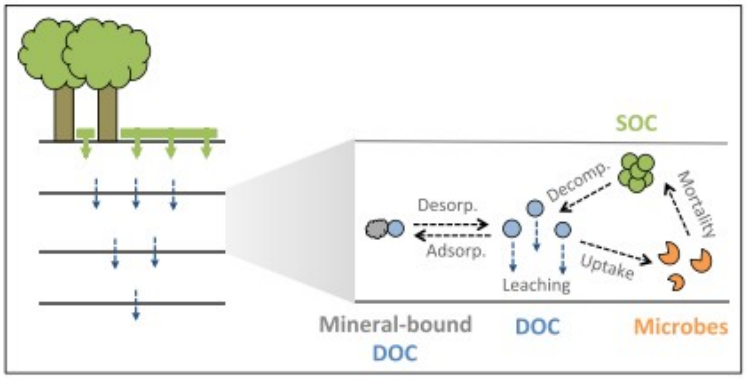

Fig. 10 Schematic of depth-resolved soil carbon cycling with dissolved organic carbon (DOC) leaching vertically through the soil profile while undergoing various chemical (i.e., desorption and adsorption with minerals) and biological (e.g., decomposition and uptake by microbial and enzymatic activity) reactions. The key constituents depicted and modeled here in addition to DOC are mineral-bound DOC, soil organic carbon (SOC), and microbial biomass. See Eq. 15a–d for details, including the functional form and parameters of each reaction

Integrating Eq. 15a–d with MAC and FD (both with first-order integration schemes of ordinary and partial derivatives, respectively) across a range of time steps (t = 0.01, 0.05, 0.1, 0.25, 0.5) with corresponding spatial steps (x) as defined by MAC, we show the resulting transient and steady-state total soil carbon (CS + CD + CB + Cq) profiles in Fig. 11. It is clear that the MAC approaches the steady-state faster and with greater accuracy than FD. This is also illustrated in Figs. 12 and 13, where we show the percent absolute error of the MAC and FD solutions as compared to the true solution (i.e., 100·|estimated − true|/true) for a range of time steps (t). For this example, we conclude that the MAC outperforms FD in accuracy, stability, and speed, especially at larger time steps.

Table 1 The parameters of the model in Eq. 15a–d are V_{max}, K_m, $V_{max,U}$, $K_{m,U}$, k_B, ε, k_{ads}, k_{des}, q_{max}, and c and were, without a loss of generality, assumed to take the values given in the table. Here, we adopt parameters from recent publications [1, 27, 30] and recognize that in each application these values will be estimated from observations

Parameter	Description	Value
V_{max}	Maximum decomposition (depolymerization) rate	1 day^{-1}
K_m	Half-saturation constant for decomposition	250 mg g^{-1}
$V_{max,U}$	Maximum assimilation rate	0.1 day^{-1}
$K_{m,U}$	Half-saturation constant for assimilation	0.26 mg g^{-1}
k_B	Mortality rate of microbes	0.005 day^{-1}
ε	Carbon use efficiency of microbes	0.31
k_{ads}	Adsorption rate	1 (mg g^{-1})$^{-1}$ day^{-1}
k_{des}	Desorption rate	0.02 day^{-1}
q_{max}	Maximum adsorption capacity	1.5 mg g^{-1}
c	Average pore water velocity	0.5 m day^{-1}

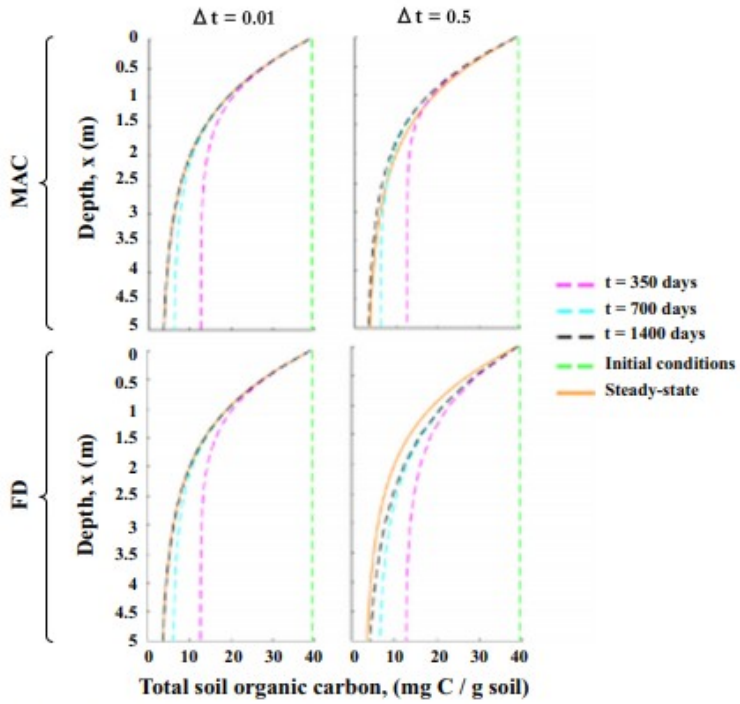

Fig. 11 Total soil organic carbon ($C_S + C_D + C_B + C_q$) profile at t = 350, 700, 1150, and 1400 days, as integrated from Eq. 15a–d with the MAC and FD for $\Delta t = 0.01$ and 0.5 days and corresponding Δx as defined by the MAC. Both the MAC and FD are implemented with first-order, implicit integration schemes of ordinary and partial derivatives, respectively, to allow for a direct comparison. Initial conditions and the steady-state solution are shown for reference

4 Discussion and concluding remarks

We have presented a method for solving systems of advection-dominated PDEs in which all partial derivatives appear in linear expressions, as in many reactive transport models. The proposed method, termed the method of alternating characteristics (MAC), is based on alternating between characteristic directions of the equations, such that a system of PDEs can be sequentially integrated, one step at a time, as ODEs along corresponding directions. We described extensions of this method to systems with two or more characteristics, spatially and temporally varying characteristics, and more than one spatial dimension. Finally, we presented two numerical examples, including applications to contaminant transport with mineral adsorption in a porous medium and to soil carbon cycling. The key is that only a subset of the chemical constituents undergoes advection, while the remaining constituents are stationary. This scenario arises naturally when a compound can be leached through a porous medium in its dissolved state, for example, but cannot be advected once adsorbed to the surrounding medium.

We compared the MAC using the first-order, implicit Euler method for ODE integration to the standard firstorder, implicit upwind finite-difference scheme for PDE integration in space and time [12, 33] and demonstrated that the MAC is substantially more accurate for a given grid resolution or simulation runtime (Fig. 8). More specifically, because the solutions of

advection-dominated PDEs are smoother along their characteristics than in the time direction, the MAC can use larger time steps while maintaining stability and accuracy. This fact is especially true for situations with steep concentration profiles. For such a case, we found that the MAC has a significant advantage in performance with regard to simulation time as well.

In implementing finite-difference schemes, we have not implemented additional advances, e.g., that improve stability [9, 18, 28, 31, 39]. Further, besides stability, when implementing finite-difference schemes, it is also important to preserve conserved quantities if that is the case [19, 26, 34]. This last point has not been considered in the current paper either. However, we anticipate that both improved stability and conservation can be suitably addressed since MAC in essence reduces to integration of ODEs. This is a topic of current interest and research.

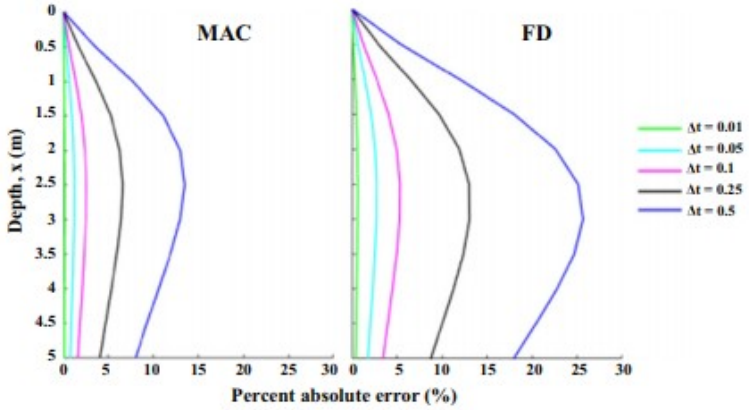

Fig. 12 Percent absolute errors obtained from comparing the MAC and FD solutions of the total soil organic carbon ($C_S + C_D + C_B + C_q$) profile to the true solution at $t = 1400$ days. The methods converge to the same solution at small enough time steps $\Delta t < 0.005$ days, and therefore, this is considered as the true solution and is used to compare the methods across increasing time steps $\Delta t = 0.01, 0.05, 0.1, 0.25$, and 0.5 days, with the corresponding Δx as defined by the MAC. Both the MAC and FD are implemented with first-order, implicit integration schemes

Our point in the present paper has been to highlight the potential advantages of the proposed method and underscore the suitability for advection-dominated environmental systems with biogeochemical reactions. We expect that the proposed MAC will be useful to other fields of study in which time-dependent advection-dominated PDEs arise, such as air pollution (e.g., atmospheric pollutant transport), geomorphology and geochemistry (e.g., sediment and contaminant transport [5, 6, 16, 41]), ecology (e.g., population densities of drift-prone aquatic species [10]), and engineering applications.

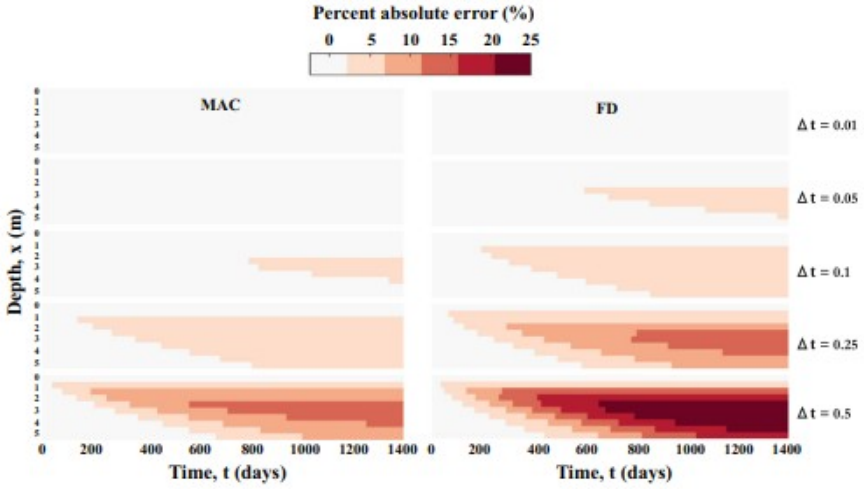

Fig. 13 Spatiotemporal evolution of percent absolute error of the first-order, implicit MAC and FD, calculated by comparing the total soil organic carbon ($C_S + C_D + C_B + C_q$) across space and time to the true solution. The two methods were implemented with time steps $\Delta t = 0.01, 0.05, 0.1, 0.25$, and 0.5 days and corresponding Δx as defined by the MAC. All solutions are shown on a $(\Delta x, \Delta t) = (0.5\text{ m}, 0.5\text{ day})$ grid for direct comparison

Acknowledgments We thank the two anonymous reviewers for their constructive input, which greatly improved this manuscript. This material is based upon work supported by the U.S. Department of Energy, Office of Science, Office of Biological and Environmental Research, as part of the Terrestrial Ecosystem Science Program under Contract No. DE-AC02-05CH11231.

Funding information K.G. acknowledges support from the National Science Foundation Graduate Research Fellowship under Grant No. DGE 1106400 and the U.S. Department of Energy, Office of Science, Office of Workforce Development for Teachers and Scientists, Office of Science Graduate Student Research (SCGSR) program. The SCGSR program is administered by the Oak Ridge Institute for Science and Education (ORISE) for the DOE. ORISE is managed by ORAU under contract number DE-SC0014664.

References

1. Ahrens, B., Braakhekke, M.C., Guggenberger, G., Schrumpf, M., Reichstein, M.: Contribution of sorption, DOC transport and microbial interactions to the 14C age of a soil organic carbon profile: insights from a calibrated process model. Soil Biol. & Biochem. 88, 390–402 (2015)

2. Allison, S.D., Wallenstein, M.D., Bradford, M.A.: Soil-carbon response to warming dependent on microbial physiology. Nature Geosci 3, 336–340 (2010)

3. Arbogast, T., Wheeler, M.F.: A characteristics-mixed finite element method for advection-dominated transport problems. SIAM J. Numer. Anal. 32, 404–424 (1995)

4. Arnold, D.N.: Stability, consistency, and convergence of numerical discretizations. Encyclopedia of App. and Comput. Mathematics, pp. 1358–1364. Springer, Berlin (2015)

5. Centler, F., Shao, H., Park, C.-H., de Biase, C., Kolditz, O., Thullner, M.: GeoSysBRNS—a flexible multi-dimensional reactive transport model for simulating biogeochemical subsurface processes. Comput. Geosci. 36, 397–405 (2010)

6. Chiang, C.Y., Wheeler, M.F., Bedient, P.B.: A modified method of characteristics technique and mixed finite elements method for simulation of groundwater solute transport. Water Resour. Res. 25, 1541–1549 (1989)

7. Douglas J., Jr: Simulation of miscible displacement in porous media by a modified method of characteristic procedure. In: Numerical analysis. Springer, Berlin, pp. 64–70 (1982)

8. Douglas J., Jr, Russell, T.F.: Numerical methods for convectiondominated diffusion problems based on combining the method of characteristics with finite element or finite difference procedures. SIAM J. Numer. Anal. 19, 871–885 (1982)

9. Donea, J., Quartapelle, L.: An introduction to finite element methods for transient advection problems. Comp. Methods App. Mech. Eng. 95, 169–203 (1992)

10. Downes, B.J., Lancaster, J.: Does dispersal control population densities in advection-dominated systems? A fresh look at critical assumptions and a direct test. Journal of Animal Ecology. 79, 235– 248 (2010)

11. Ewing, R.E.: Simulation of multiphase flows in porous media. Trans. Porous Media 6, 479–499 (1991)

12. Ewing, R.E., Wang, H.: A summary of numerical methods for time-dependent advection-dominated partial differential equations. J. Comput. Appl. Math. 128, 423–445 (2001)

13. Ewing, R.E., Russell, T.F., Wheeler, M.F.: Convergence analysis of an approximation of miscible displacement in porous media by mixed finite elements and a modified method of characteristics. Comput. Methods Appl. Mech. Eng. 47, 73–92 (1984)

14. Fang, Y.L., Yabusaki, S.B., Yeh, G.T.: A general simulator for reaction-based biogeochemical processes. Comput. Geosci. 32, 64–72 (2006)

15. Frei, S., Knorr, K.H., Peiffer, S., Fleckenstein, J.H.: Surface micro-topography causes hot spots of biogeochemical activity in wetland systems: a virtual modeling experiment. J. of Geophys. Res. 117, 1–18 (2012)

16. Gruber, J.: Contaminant accumulation during transport through porous media. Water Resour. Res. 26, 99–107 (1990)

17. Hararuk, O., Smith, M.J., Luo, Y.: Microbial models with datadriven parameters predict stronger soil carbon responses to climate change. Global Change Biol 21, 2439–2453 (2015)

18. Harten, A., Engquist, B., Osher, S., Chakravarthy, S.R.: Uniformly high order accurate non-oscillatory schemes, III. J. of Comput. Phys. 71, 231–303 (1987)

19. Ham, F.E., Lien, F.S., Strong, A.B.: A fully conservative secondorder finite difference scheme for incompressible flow on nonuniform grids. J. of Comput. Phys. 177, 117–133 (2002)

20. Holstad, A.: A mathematical and numerical model for reactive fluid flow systems. Comput. Geosci. 4, 103–139 (2000)

21. Knabner, P.: Finite-element-approximation of solute transport in porous media with general adsorption processes. In: Xiao, S.- T. (ed.) Flow and transport in porous media, pp. 223-292. World Scientific, Singapore (1992)

22. Knabner, P., Totsche, K.U., Kogel-Knabner, I.: The modeling of ¨ reactive solute transport with sorption to mobile and immobile sorbents. 1. Experimental evidence and model development. Water Resour. Res. 32, 1611–1622 (1996)

23. Knabner, P., Igler, B.A., Totsche, K.U., DuChateau, P.: Unbiased identification of nonlinear sorption characteristics by soil column breakthrough experiments. Comput. Geosci. 9, 203–217 (2005)

24. Lakoba, T.: Method of characteristics for solving hyperbolic PDEs, University of Vermont. http://www.cems.uvm.edu/ ~tlakoba/math337/notes 17.pdf. Accessed 11 April 2016

25. Lele, S.K.: Compact finite difference schemes with spectral-like resolution. J. of Comput. Phys. 103, 16–42 (1992)

26. Leveque, R.: Finite volume methods for hyperbolic problems. Cambridge University Press, Cambridge (2002)

27. Li, J., Wang, G., Allison, S.D., Mayes, M.A., Luo, Y.: Soil carbon sensitivity to temperature and carbon use efficiency compared across microbial-ecosystem models of varying complexity. Biogeochem. 119, 67–84 (2014)

28. Liu, X.D., Osher, S., Chan, T.: Weighted essentially nonoscillatory schemes. J. of Comput. Phys. 115, 200–212 (1994)

29. Matzner, E., Zuber, T., Alewell, C., Lischeid, G., Moritz, K.: Trends in deposition and canopy leaching of mineral elements as indicated by bulk deposition and throughfall measurements. In: Matzner, E. (ed.) Biogeochemistry of forested catchments in a changing environment, pp. 233–250. Springer, Berlin (2014)

30. Mayes, M.A., Heal, K.R., Brandt, C.C., Phillips, J.R., Jardine, P.M.: Relation between soil order and sorption of dissolved organic carbon in temperate subsoils. Soil Sci. Soc. Am. J. 76, 1027–1037 (2011)

31. Mazzia, A., Putti, M.: High order Godunov mixed methods on tetrahedral meshes for density driven flow simulations in porous media. J. of Comput. Phys. 208, 154–174 (2005)

32. Meysman, F.J.R., Boudreau, B.P., Middelburg, J.J.: Modeling reactive transport in sediments subject to bioturbation and compaction. Geochimica et Cosmochimica Acta 69, 3601–3617 (2005)

33. Olver, P.J.: Introduction to partial differential equations, Chapters 2 and 5. Springer, Berlin (2014)

34. Osher, S., Solomon, F.: Upwind difference schemes for hyperbolic systems of conservation laws. Mathematics of Comput 38, 339–374 (1982)

35. Russel, T.F., Wheeler, M.F.: Finite element and finite difference methods for continuous flow in porous media. In: Ewing, R.E. (ed.) The mathematics of reservoir simulation, pp. 35–106. SIAM, Philadelphia (1984)

36. Riley, W.J., Maggi, F., Kleber, M., Torn, M.S., Tang, J.Y., Dwivedi, D., Guerry, N.: Long residence times of rapidly decomposable soil organic matter: application of a multi-phase, multi-component, and vertically resolved model (BAMS1) to soil carbon dynamics. Geosci. Model Dev 7, 1335–1355 (2014)

37. Rinaldo, A., Beven, K.J., Bertuzzo, E., Nicotina, L., Davies, J., Fiori, A., Russo, D., Botter, G.: Catchment travel time distributions and water flow through in soils. Water Resour. Res. 47, 1–13 (2011)

38. Scovazzi, G., Wheeler, M.F., Mikelic, A., Lee, S.: Analytical and ´ variational numerical methods for unstable miscible displacement flows in porous media. J. of Comput. Phys. 335, 444–496 (2017)

39. Shu, C.W., Osher, S.: Efficient implementation of essentially nonoscillatory shock-capturing schemes. J. of Comput. Phys. 77, 439– 471 (1988)

40. Sinsabaugh, R.L., Mazoni, S., Moorhead, D.L., Richter, A.: Carbon use ef? ciency of microbial communities: stoichiometry, methodology and modelling. Ecology Lett. 16, 930–939 (2013)

41. Steefel, C.I., DePaolo, D., Lichtner, P.C.: Reactive transport modeling: an essential tool and a new research approach for the Earth sciences. Earth Planet Sci. Lett. 240, 539–558 (2005)

42. Steefel, C.I., Appelo, C.A.J., Arora, B., et al.: Reactive transport codes for subsurface environmental simulation. Comput. Geosci. 19, 445–478 (2015)

43. Strikwerda, J.C.: Finite difference schemes and partial differential equations. Wadsworth and Brooks/Cole, Pacific Grove (1989)

44. Tadmor, E.: A review of numerical methods for nonlinear partial differential equations. Bull. Am. Math. Soc. 49, 507–554 (2012)

45. Tang, J.Y., Riley, W.J., Koven, C.D., Subin, Z.M.: CLM4-BeTR, a generic biogeochemical transport and reaction module for CLM4: model development, evaluation, and application. Geosci. Model Dev 6, 127–140 (2013)

46. Todd-Brown, K.E.O., et al.: Changes in soil organic carbon storage predicted by Earth system models during the 21st century. Biogeosci 11, 2341–2356 (2014)

47. Weill, S., Mazzia, A.M., Putti, M., Paniconi, C.: Coupling water flow and solute transport into a physically-based surface–subsurface hydrological model. Adv. in Water Res 34, 128–136 (2011)

48. Wieder, W.R., Allison, S.D., Davidson, E.A., et al.: Explicitly representing soil microbial processes in Earth system models. Global Biogeochem. Cycles. 29, 1782–1800 (2015)

49. Wiggert, D.C., Wylie, E.B.: Numerical predictions of twodimensional transient groundwater flow by the method of characteristics. Water Resour. Res. 12, 971–977 (1976)